7. Bowring R. W. Physical Model Based on Bubble Detachment and Calculation of Steam Voidage in the Subcooled Region of a Heated Channel. *HPR-10, Institutt for Atomenergi*, Halden, Norway, 1962.
8. Engelberg-Forster K. Heat transfer to a boiling liquid - mechanism and correlations. *Trans. ASME J. Heat Transfer.* 1959. Ser. C. No. 81. P. 43–53.
9. Rohsenow W. M. A method of correlating heat transfer data for surface boiling of liquids. *Trans. ASME J. Heat Transfer.* 1952. No. 74. P. 969.
10. Bergles A. E. The determination of forced convection surface boiling heat transfer. *Proc. of 6th National Heat Transfer Conf.* August 11–14, 1963. Boston, USA. ASME Paper 63-HT-22.
11. Kandlikar S. G. Heat Transfer Characteristics in Partial Boiling, Fully Developed Boiling, and Significant Void Flow Regions of Subcooled Flow Boiling. *J. Heat Transfer.* 1998. Vol. 120. P. 395–401. https://doi.org/10.1115/1.2824263
12. Hsu Y. Y. On the Size Range of Active Nucleation Cavities on a Heating Surface. *ASME J. Heat Transfer.* 1962. Vol. 84. P. 207–216. https://doi.org/10.1115/1.3684339
13. Sato T. On the Conditions of Incipient Subcooled Boiling with Forced Convection. *Bulletin JSME.* 1964. Vol. 7. No. 26. P. 392–398. https://doi.org/10.1299/jsme1958.7.392


**DOI: https://doi.org/10.15407/pmach2019.01.016**

UDC 539.3

# STRESSED STATE OF A HOLLOW CYLINDER WITH A SYSTEM OF CRACKS UNDER LONGITUDINAL SHEAR HARMONIC OSCILLATIONS

**Olga I. Kyrylova**
olga.i.kyrylova@gmail.com
ORCID: 0000-0002-9221-182X

**Vsevolod H. Popov**
dr.vg.popov@gmail.com
ORCID: 0000-0003-2416-642X

National University
"Odessa Maritime Academy",
8, Didrikhson St., Odesa,
65029, Ukraine

*This paper solves the problem of determining the stress state near cracks in an infinite hollow cylinder of arbitrary cross section during longitudinal shear oscillations. We propose an approach that allows us to separately satisfy conditions both on the cracks and boundaries of a cylinder. The problem reduces to the equations of motion in a flat domain with the defects bounded by arbitrary smooth closed curves under anti-plane deformation conditions. The solution scheme is based on the use of discontinuous solutions to the equations of motion of an elastic medium with displacement jumps on the surfaces of defects. Displacements in a cylinder with defects are represented both as a sum of discontinuous solutions constructed for each defect and an unknown specific function ensuring that the conditions of a harmonic load on the body boundaries are met. This function is sought as a linear combination of linearly independent solutions to the equations of the theory of elasticity in the frequency domain with unknown coefficients. The constructed representation makes it possible to separately satisfy the boundary conditions on the surfaces of defects, which results in a set of systems of integral equations that differ only in their right-hand sides and do not depend on the body boundary shape. The resulting systems of integral equations can be solved by the method of mechanical quadratures. After that, the conditions on the boundaries of the cylindrical body are satisfied, from which the unknown coefficients of the introduced specific function are determined by a collocation method. Using the approach proposed, the stress intensity factors in the vicinity of defects were calculated. With the help of those calculations, we investigated the effect of the frequency and location of the defects on the stress intensity coefficient values.*

***Keywords:*** *hollow cylinder, harmonic oscillations, stress intensity factors, system of cracks.*

## Introduction

Investigation of the stress state of the bounded bodies with cracks is relevant both for determining the conditions for the destruction of the bodies by estimating the coefficients of the intensity of dynamic stresses in the vicinity of cracks and diagnosing such defects based on the information on their effect on resonance frequencies. The results obtained in this direction related mainly to both unbounded and semi-bounded defective bodies [1-4]. A much smaller number of situations have been considered for the cases where the bodies occupy limited areas. This is due to the fact that with the application of the method of boundary integral equations, the original problems are reduced to the interrelated systems of integral equations given on both the defect surface and boundary of the body [5–7], which significantly complicates the numerical implementation, especially in the case of uncommon defects and multi-connected domains. This paper proposes a method that allows the boundary conditions on the defects and surface of a body to be independently and consistently satisfied.

**Problem Formulation**

A hollow elastic cylinder is considered, with its elements being parallel to the $Oz$ axis, and the $xOy$ cross-section being a two-connected plane domain bounded by arbitrary closed smooth curves. These curves are in the polar coordinate system whose center coincides with the origin of the $xOy$ coordinates, and are determined by the equations: $r = r_0\psi_0(\phi)$ for the external boundaries and $r = r_1\psi_1(\phi)$ for the internal ones, $0 \le \phi < 2\pi$. The cylinder contains $N$ through cracks with centers at the points $(c_k, d_k)$, that in the $xOy$ plane do not extend beyond the cross-section and occupy $2a_k, k = \overline{1,N}$ long segments (Fig. 1).

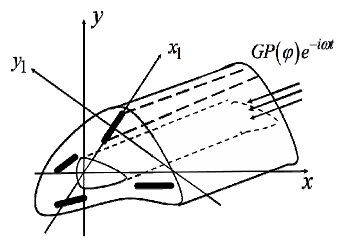


***Fig.1 Infinite hollow cylinder with cracks***

In the cylinder, longitudinal shear oscillations occur. They result from the lateral surface being under the action of the self-equilibrium harmonic load $GP(\phi)e^{-i\omega t}$, where $G$ – the shear modulus, $P(\phi)$ – the given non-dimentional load amplitude, $\omega$ – the oscillation frequency. The multiplier $e^{-i\omega t}$ is omitted everywhere. Under such conditions, other than zero is only the $z$-component of the displacement vector, with the component satisfying the Helmholtz equation [8]. In the polar system, this equation has the form:

$$\Delta w + \kappa_2^2 w = 0; \quad \Delta = \frac{\partial^2}{\partial r^2} + \frac{1}{r}\frac{\partial}{\partial r} + \frac{1}{r^2}\frac{\partial^2}{\partial \phi^2}, \tag{1}$$

where $\kappa_2 = \dfrac{\omega}{C_2}$; $C_2 = \sqrt{\dfrac{G}{\rho}}$; $\rho$ is the density of the cylinder material.

The outer surface of the cylinder is considered to be loaded:

$$\tau_{\bar{n}z}(r_0\psi_0(\phi), \phi) = GP(\phi), 0 \le \phi < 2\pi, \tag{2}$$

The interior surface is considered to be motionless:

$$w(r_1\psi_1(\phi), \phi) = 0, 0 \le \phi < 2\pi. \tag{3}$$

In order to formulate the boundary conditions at cracks, each of the crack centers is associated with the local coordinate system $x_k O_k y_k, k = \overline{1,N}$ (Fig. 1). The relationship between the local and global systems is given by the formulas:

$$\begin{cases} x = c_k + x_k\cos\alpha_k - y_k\sin\alpha_k, \\ y = d_k + x_k\sin\alpha_k + y_k\cos\alpha_k. \end{cases} \tag{4}$$

$$\begin{cases} x_l = (c_k - c_l)\cos\alpha_l + (d_k - d_l)\sin\alpha_l + x_k\cos(\alpha_k - \alpha_l) - y_k\sin(\alpha_k - \alpha_l), \\ y_l = -(c_k - c_l)\sin\alpha_l + (d_k - d_l)\cos\alpha_l + x_k\sin(\alpha_k - \alpha_l) + y_k\cos(\alpha_k - \alpha_l), \end{cases} \quad k, l = 1,2,...N.$$

The relationship between the local and polar coordinate systems has the form:

$$\begin{cases} x_l = (r\cos\phi - c_l)\cos\alpha_l + (r\sin\phi - d_l)\sin\alpha_l, \\ y_l = (r\sin\phi - d_l)\cos\alpha_l - (r\cos\phi - c_l)\sin\alpha_l. \end{cases} \tag{5}$$

Let $w_k(x_k, y_k)$ be a $z$-component of the displacement vector in the conversion from Polar to Cartesian coordinates by formulas (5). Cracks are considered to be free of loads:

$$\tau_{zy_k}(x_k, 0) = G\frac{\partial w_k}{\partial y_k}(x_k, 0) = 0, \ |x_k| < a_k, \ k = \overline{1,N}. \tag{6}$$

Also, on crack surfaces, there are discontinuous displacements with jumps

$$\langle w_k \rangle = w_k(x_k, +0) - w_k(x_k, -0) = \chi_k(x_k), \ |x_k| < a_k, k = \overline{1,N}. \tag{7}$$

From the conditions for crack closure, it follows that $\chi_k(\pm a_k) = 0$.

Under these conditions, a problem of determining the stress state in the vicinity of cracks is assigned.

**Solving the Problem**

For each crack in the local coordinate system, a discontinuous solution [9] with jumps (7) is constructed:

$$w_l^{(d)}(x_l, y_l) = \frac{\partial}{\partial y_l}\int_{-a_l}^{a_l}\chi_l(\eta) r_2(\eta - x_l, y_l) d\eta, \tag{8}$$

where $r_2(\eta - x_l, y_l) = -\frac{i}{4} H_0^{(1)}\left(\kappa_2\sqrt{(\eta - x_l)^2 + y_l^{\,2}}\right)$, $H_0^{(1)}$ is the Hankel function.

Further, in the Polar coordinate system, the displacement is presented as:

$$w^{(g)}(r,\phi) = w_0^{(g)}(r,\phi) + \sum_{l=1}^{N} w_l^{(g)}(r,\phi), \tag{9}$$

where $w_l^{(g)}(r,\phi)$ are discontinuous solutions (8) after the conversion to polar coordinates, $w_0^{(g)}(r,\phi)$ is some unknown function, which is the solution to the Helmholtz equation (1) through which conditions (2), (3) on the cylinder surface will be met.

Next, this function is presented as a linear combination of partial solutions to the Helmholtz equation (1):

$$w_0^{(g)}(r,\phi) = r_0\sum_{s=1}^{M}\left(A_s g_s(r,\phi) + B_s h_s(r,\phi)\right) \tag{10}$$

where

$$h_{2m-1}(r,\phi) = H_{m-1}(\kappa_2 r)\cos(m-1)\phi,\; h_{2m}(r,\phi) = H_m(\kappa_2 r)\sin m\phi;$$

$$g_{2m-1}(r,\phi) = J_{m-1}(\kappa_2 r)\cos(m-1)\phi,\; g_{2m}(r,\phi) = J_m(\kappa_2 r)\sin m\phi\,.$$

These functions are linearly independent and form a complete closed system in the cross-section [10].

In order to realize boundary conditions (6) at the cracks in the coordinate system associated with the $k^{\text{th}}$ crack, the displacement is given similarly to (9)

$$w_k(x_k, y_k) = w_k^0(x_k, y_k) + \sum_{l=1}^{N} w_k^l(x_k, y_k) \tag{11}$$

where $w_k^0(x_k, y_k)$ is obtained from $w_0^{(g)}(r,\phi)$ after the conversion of coordinates by (5), and $w_k^l(x_k, y_k)$ as a result of substitution into $w_l^{(g)}(r,\phi)$ $x_l, y_l$ by the second formulas in (4).

Thereafter, the substitution of (11) into (6) leads to a system of integro-differential equations, which, after separating the singular components, takes the form:

$$\frac{1}{2\pi}\int_{-1}^{1}\left(\phi_{sk}^{(i)}(\tau)\right)'\left[\frac{1}{\tau-\varsigma} + R_k^{(1)}(\tau-\varsigma)\right]d\tau + \frac{1}{2\pi}\int_{-1}^{1}\phi_{sk}^{(i)}(\tau)\left[-\gamma_k^2\kappa_0^2\ln|\tau-\varsigma| + R_k^{(0)}(\tau-\varsigma)\right]d\tau +$$
$$+\sum_{\substack{l=1\\ l\neq k}}^{N}\left[\frac{1}{2\pi}\int_{-1}^{1}\left(\phi_{sl}^{(i)}(\tau)\right)' F_{kl}^{(1)}(\tau,\varsigma)d\tau + \frac{1}{2\pi}\int_{-1}^{1}\phi_{sl}^{(i)}(\tau)F_{kl}^{(0)}(\tau,\varsigma)d\tau\right] = f_{sk}^{(i)}(\varsigma), \tag{12}$$

$$k = 1,\ldots,N;\; s = 1,..M;\;\; i = 1,2.$$

The kernels of the integral operators $F_{kl}^{0}(\tau,\varsigma)$, $F_{kl}^{(1)}(\tau,\varsigma)$ are the functions that are infinitely differentiable with $-1 \le \tau,\varsigma < 1$, while for others, there occurs the asymptotic behavior:

$$R_k^{(1)}(z) = O\left(z\ln|z|\right),\quad R_k^{(0)}(z) = O\left(z^2\ln|z|\right),\quad z \to 0$$

The right-hand sides in (12) are equal to

$$f_{sk}^{(1)}(\varsigma) = -r_0\frac{\partial g_s(a_k\varsigma,0)}{\partial y_k};\; f_{sk}^{(2)}(\varsigma) = -r_0\frac{\partial h_s(a_k\varsigma,0)}{\partial y_k}.$$

When deriving system (12), we used the representations:

$$\kappa_0 = \kappa_2 r_0,\ \gamma_k = \frac{a_k}{r_0},\ \eta = a_k \tau,\ x_k = a_k \varsigma,\ c_k^0 = \frac{c_k}{r_0},\ d_k^0 = \frac{d_k}{r_0},$$

$$\alpha_{kl} = a_k - \alpha_l,\ a_l \phi_l(\tau) = \chi_l(a_l \tau),\ \chi_l'(a_l \tau) = \phi_l'(\tau).$$

In addition, due to linearity (12), we gave the unknown functions as:

$$\begin{aligned} \phi_l(\tau) &= a_l \sum_{s=1}^{M} \left( A_s \phi_{sl}^{(1)}(\tau) + B_s \phi_{sl}^{(2)}(\tau) \right), \\ \phi_l'(\eta) &= \sum_{s=1}^{M} \left( A_s \left( \phi_{sl}^{(1)}(\tau) \right)' + B_s \left( \phi_{sl}^{(2)}(\tau) \right)' \right). \end{aligned} \tag{13}$$

To (12) we should add another equality, which results from the conditions for crack closure:

$$\int_{-1}^{1} \left( \phi_{sk}^{(i)}(\tau) \right)' d\tau = 0 \tag{14}$$

The solution to integral equations (12), (14) is based on the representation of the derivatives of the unknown functions in form [11]:

$$\left( \phi_{sk}^{(i)}(\tau) \right)' = \frac{\psi_{sk}^{(i)}(\tau)}{\sqrt{1-\tau^2}},\ k = 1,2,\ldots,N \tag{15}$$

and approximation of the functions $\psi_{sk}^{(i)}(\tau)$ by the following interpolation polynomial

$$\psi_{sk}^{(i)}(\tau) = \sum_{m=1}^{n} \left( \psi_{sk}^{(i)} \right)_m \frac{T_n(\tau)}{(\tau - \tau_m) T_n'(\tau_m)}, \tag{16}$$

where $T_n(\tau)$ is the Chebyshev polynomial, $\tau_m$ are its roots, $\left( \psi_{sk}^{(i)} \right)_m = \psi_{sk}^{(i)}(\tau_m)$.

As shown in [4], from formulas (15), (16) for $\phi_{sk}^{(i)}(\tau)$ the following approximation is derived:

$$\phi_{sk}^{(i)}(\tau) = \sqrt{1-\tau^2} \left( L_{sk}^{(i)} \right)_n, \left( L_{sk}^{(i)} \right)_n (\tau) = -\frac{2}{n} \sum_{m=1}^{n} \left( \psi_{sk}^{(i)} \right)_m \sum_{p=1}^{n-1} \frac{T_p(\tau_m) U_{p-1}(\tau)}{p} \tag{17}$$

Formulas (15) and (17) give us the opportunity to solve the equations by the method of mechanical quadratures using the roots of the Chebyshev polynomial $U_{n-1}(\varsigma) : \varsigma_j = \cos\frac{\pi j}{n}, j = 1,2,\ldots,n-1$ as collocation points. In applying this method, for the Cauchy integrals, the well-known quadrature formula [11] is used, for the integrals with regular nuclei, the Gauss-Chebyshev formulas are used. The integral with logarithmic singularity is calculated by the formula obtained from [4]:

$$\int_{-1}^{1} \phi_s^k(\tau_m) \ln\left| \tau_m - \varsigma_j \right| d\tau = \sum_{m=1}^{n} a_m \psi_{sm}^k C_{jm},\ \ k = 1,\ldots,n;\ j = 1,\ldots,n-1,$$

$$C_{jm} = \tau_m \left( \ln 2 - \frac{1}{2} \cos 2\sigma_j \right) - 2 \sum_{p=2}^{n-1} \frac{\cos(p\beta_m)}{p} \left( \cos(p-1)\sigma_j - \frac{\cos(p+1)\sigma_j}{p+1} \right),$$

$$\beta_m = \frac{(2m-1)\pi}{2n};\ \sigma_j = \frac{j\pi}{n};\ a_m = \frac{\pi}{n}.$$

As a result, a set of well-defined systems of linear equations with respect to the node values $\left( \psi_{sk}^{(i)} \right)_m$ is obtained:

$$\frac{1}{2\pi}\sum_{m=1}^{n}a_m\left(\psi_{sk}^{(i)}\right)_m\left[\frac{1}{\tau_m-\varsigma_j}+R_{jm}^{k}\right]+\frac{1}{2\pi}\sum_{m=1}^{n}a_m\left(\psi_{sk}^{(i)}\right)_m\left[-\gamma_k^2\kappa_0^2C_{jm}+D_{jm}^{k}\right]+$$
$$+\frac{1}{2\pi}\sum_{\substack{l=1\\l\neq k}}^{N}\left[\sum_{m=1}^{n}a_m\left(\psi_{sl}^{(i)}\right)_m F_{jm}^{kl}+\sum_{m=1}^{n}a_m\left(\psi_{sl}^{(i)}\right)_m E_{jm}^{kl}\right]=f_{sk}^{(i)}\left(\varsigma_j\right), \tag{18}$$
$$\sum_{m=1}^{n}a_m\left(\psi_{sk}^{(i)}\right)_m=0.$$
$$j=1,...,n-1;\quad k=1,...,N;\quad s=1,...,M,\quad i=1,2.$$

In (18)

$$R_{jm}^{k}=R_k^{(1)}\left(\tau_m-\varsigma_j\right),\quad F_{jm}^{kl}=F_{kl}^{(1)}\left(\tau_m-\varsigma_j\right),\quad D_{jm}^{(k)}=\sum_{r=1}^{n}B_{sm}R_k^{0}(z_r-\varsigma_j),\quad E_{jm}^{kl}=\sum_{r=1}^{n}B_{rm}F_{kl}^{0}(z_r-\varsigma_j),$$

$$B_{rm}=-\frac{2}{n+1}\sin\frac{r\pi}{n+1}\sum_{p=1}^{n-1}\frac{\cos(p\beta_m)\sin(p\rho_r)}{p},\quad \beta_m=\frac{(2n-1)\pi}{2n},\ \rho_s=\frac{s\pi}{n+1},\ z_s=\cos\rho_s.$$

The unknown coefficients $A_k$, $B_k$ in (10) are determined from conditions (2), (3) at the boundaries of the cylinder. To implement (2), we calculate the stress

$$\tau_{\bar{n}z}\left(r_0\psi(\phi),\phi\right)=\tau_{xz}\left(r_0\psi(\phi),\phi\right)c_x+\tau_{yz}\left(r_0\psi(\phi),\phi\right)c_y. \tag{19}$$

In formula (19), $c_x, c_y$ are the directional cosines of the normal vector.

After substituting the expressions found for the stress into (19), boundary condition (2) takes the form:

$$\sum_{s=1}^{M}A_s\left(\sum_{k=1}^{N}\int_{-1}^{1}\phi_{sk}^{(1)}(\tau)G_k(\tau,\phi)d\tau+F_s^{(1)}(\phi)\right)+\sum_{s=1}^{M}B_s\left(\sum_{k=1}^{N}\int_{-1}^{1}\phi_{sk}^{(2)}(\tau)G_k(\tau,\phi)d\tau+F_s^{(2)}(\phi)\right)=P(\phi) \tag{20}$$

Condition on the inner surface (3), after the unknown functions are presented as in (13), will look like:

$$\sum_{s=1}^{M}A_s\left(\sum_{k=1}^{N}\int_{-1}^{1}\phi_{sk}^{(1)}(\tau)U_k(\tau,\phi)d\tau+g_s\left(r_1\psi_1(\phi),\phi\right)\right)+\sum_{s=1}^{M}B_s\left(\sum_{k=1}^{N}\int_{-1}^{1}\phi_{sk}^{(2)}(\tau)U_k(\tau,\phi)d\tau+h_s\left(r_1\psi_1(\phi),\phi\right)\right)=0. \tag{21}$$

Approximation (17) makes it possible to replace the integrals in (20), (21) with integral sums using the Gauss-Chebyshev quadrature formula, after which, by applying the method of collocation in the nodes $\sigma_r=\dfrac{2\pi r}{M}$, $r=1,..,M$ from (20), (21), we obtain a system of $2M$ linear equations to determine $A_s$ and $B_s$.

The values that determine the possibility of crack development are the stress intensity factors (SIFs) at the vertices $x_l=\pm a_l$, which in this case are determined by the formulas:

$$K_l^{\pm}=\sqrt{a_l}\lim_{\varsigma\to\pm1\pm0}\sqrt{\varsigma^2-1}\,\tau_{y_lz}(a_l\tau,0)$$

After solving both (18) and the system obtained after the boundary conditions are satisfied, SIFs have the dimensionless values obtained:

$$k_l^{\pm}=\frac{K_l^{\pm}}{G\sqrt{a_l}}=\frac{(-1)^{n+1}}{2n}\left(\sum_{s=1}^{M}A_s\sum_{m=1}^{n}(-1)^m\psi_{sm}^{(1l)}\left(\mathrm{ctg}\frac{\gamma_m}{2}\right)^{\pm1}+\sum_{s=1}^{M}B_s\sum_{m=1}^{n}(-1)^m\psi_{sm}^{(2l)}\left(\mathrm{ctg}\frac{\gamma_m}{2}\right)^{\pm1}\right),$$

where $\gamma_m=\dfrac{\pi(2m-1)}{2n}$.

**Results of Numerical Studies**

As an example, a cylinder with a cross-section bounded by two ellipses was considered (Fig. 2).

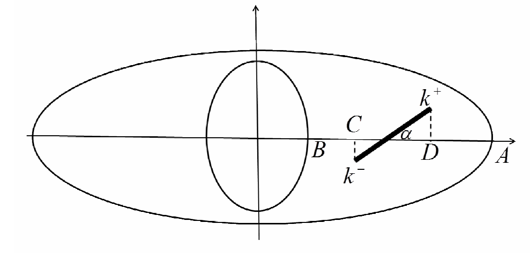


***Fig.2. Cross-section of a cylinder with a crack***

It was considered that the external boundary is under load $P(\phi)=\sin 2\phi$, the eccentricities of the inner and outer ellipses are identical and equal ε=0.5, the ratio of the semisolid of the ellipses $r_1/r_0=0.5$.

First, we investigated the dependence of the absolute SIF values on the dimensionless wave number $\kappa_0=\kappa_2 r_0$ for different angles of the crack in relation to the surfaces of the body. Fig. 3 corresponds to the case of an inclined crack with a fixed length equal to one third of the distance between the vertices of the ellipses $AB$ and the center of the crack at an equal distance from the cross-section. Curves 1–5 illustrate the behavior of SIFs for angles of $0^0, 30^0, 45^0, 60^0, 90^0$, respectively. As the analysis of calculations has shown, the behavior of SIFs is identical for both crack vertices, but $|k^-|<|k^+|$. In view of this, the results of numerical studies of the behavior of the SIF absolute values in the frequency domain, in particular their achieving the resonance regime, are given for $|k^+|$ (Fig. 3).

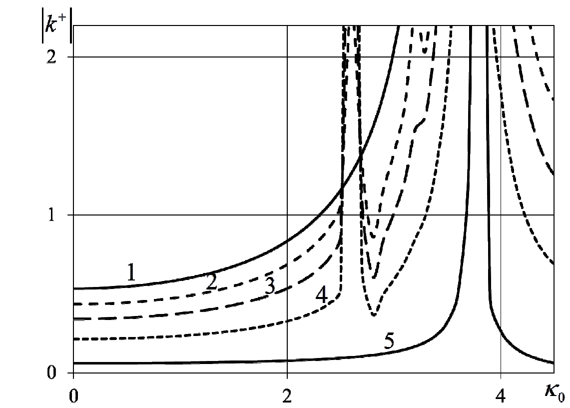


***Fig. 3. Dependence of the SIF behavior on frequency when the crack inclination angle changes***

Before reaching the first resonance frequency, SIFs decrease as the crack inclination angle increases. The inclination angle also significantly affects the number and value of resonant frequencies. So, for the inclination angles $\alpha=0^0$ and $\alpha=90^0$ there is no resonance at $\kappa_0\approx 2.6$ that can be observed for other angle inclination values. However, all the cases considered are characterized by the SIF resonant behavior when $\kappa_0\approx 3.8$.

Fig. 4. shows SIF behavior dependence on frequency with the increase in the relative crack length when the vertex approaches cylinder boundaries. Fig. 4, a corresponds to a crack along the axis of abscissa $(\alpha=0^0)$ with a variable length, so that the left end of the crack *C* was fixed, and the right one *D* approached the outer edge of the cross-section. That was achieved by changing the parameter $\gamma=a/r_0$ from 0.094 to 0.189 when the crack reached the outer surface. Curves 1, 2, 3 correspond to the values of $\gamma=0.094$; 0.141; 0.188.

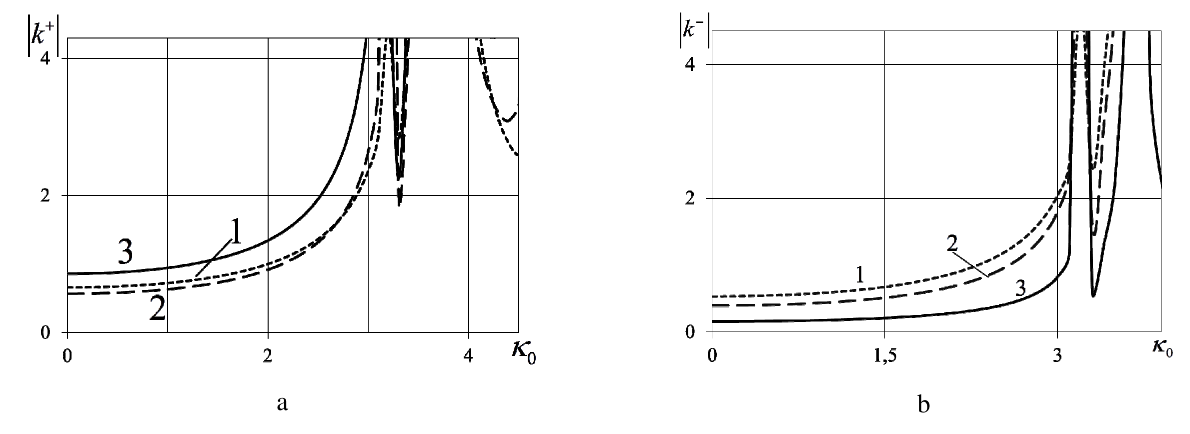


***Fig. 4 Dependence of the SIF behavior on frequency with the increase in the relative crack length:***
a – when the vertex approaches the top to the loaded surface; b – when the vertex approaches the motionless (inner) surface

It turned out that such a parametrization almost does not affect the absolute SIF values $\left|k^{-}\right|$ in the vertex of the crack $S$ that is distant from the crack outer contour. In the case considered, SIFs $\left|k^{+}\right|$ increase as the relative crack length increases and the vertex approaches the outer boundary of the cylindrical body. Resonance phenomena can be observed in the frequency range of $3 < \kappa_0 < 4$ (Fig. 4, a).

Fig. 4, b shows the SIF behavior for the same crack in the case when the right end was fixed, and the left one approached the inner surface at the same values $\gamma$. It turned out that such a parametrization affects the behavior of $\left|k^{-}\right|$, while for $\left|k^{+}\right|$ the values are almost unchanged.

As the crack length increases and approaches the inner boundary of the cylindrical body, in contrast to similar results for the crack end approaching the outer boundary (Fig. 4, a), the absolute SIF values decrease. Resonant phenomena can be observed, as in the previous case, in the frequency range of $3 < \kappa_0 < 4$ (Fig. 4, b).

## Conclusions

We propose an effective analytical-numerical method for the determination of dynamic stresses in a hollow cylindrical body of arbitrary cross-section with transverse cracks for antiplane deformation. It allows us to separately solve the integral equations at the defect and satisfy the conditions at the body boundary, thus facilitating the numerical implementation.

The method can be generalized to the case of a flat deformation state. This is confirmed by the results of [12], [13], where such problems are solved for a cylindrical body, whose cross-section is a simply connected domain. Certain difficulties in applying this method arise when the defect approaches the cylinder outer boundary. But in general, the proposed method allows us to approximately calculate SIFs and investigate how their values are effected by the geometric parameters of the crack and cylinder in a rather wide frequency range.

It is shown that the presence of cracks in an elastic hollow cylinder under harmonic load is accompanied by both the intensity of dynamic stresses in the vicinity of defects and the resonance nature of their change due to the generation of the wave process in the limited region.

In the frequency range considered, it is possible to achieve one or two resonances, depending on the crack inclination angle in relation to the body boundary. The change in the inclination angle, as well as the crack approaching the outer surface, significantly affect both the SIF value and speed of their achieving the resonance regime from the low-frequency domain.

## References


1. Popov, V. G. (1995). *Sravnitelnyy analiz difraktsionnykh poley pri prokhozhdenii uprugikh voln cherez defekty razlichnoy prirody* [Comparative analysis of diffraction fields during the passage of elastic waves through defects of different nature]. *Izv. RAN Mekhanika tverdogo tela – Mechanics of Solids,* no. 4, pp. 99–109 (in Russian).
2. Ang, D. D. & Knopoff, L. (1964). Diffraction of scalar elastic waves by a finite strip. *Proc. Math. Sci. USA*, vol. 51, no. 4, pp. 593–598. https://doi.org/10.1073/pnas.51.4.593
3. Mykhas'kiv, V., Zhbadynskyi, I., & Zhang, Ch. (2010). Elastodynamic analysis of multiple crack problem in 3-D bi-materials by a BEM. *Int. J. Num. Meth. Biomed. Eng.*, vol. 26, no. 12, pp. 1934–1946. https://doi.org/10.1002/cnm.1285
4. Popov, V. G. (1999). *Vzaimodeystviye ploskikh uprugikh voln s sistemami radialnykh defektov* [Interaction of plane elastic waves with systems of radial defects]. *Izv. RAN Mekhanika tverdogo tela – Mechanics of Solids,* no. 4, pp. 118–129 (in Russian).
5. Chirino, F. & Domingues, J. (1989). Dynamic analysis of cracks using boundary element method. *Engineering Fracture Mechanics*, vol. 34, no. 5–6, pp. 1051–1061. https://doi.org/10.1016/0013-7944(89)90266-X
6. Bobylev, A. A. & Dobrova Yu. A. (2003). *Primeneniye metoda granichnykh elementov k raschetu vynuzhdennykh kolebaniy uprugikh tel konechnykh razmerov s treshchinami* [Application of the boundary element method to the calculation of forced vibrations of finite-sized elastic bodies with cracks]. *Vestnik Khark. nats. un-ta – Bulletin of Kharkov National University*, no. 590, iss. 1, pp. 49–54 (in Russian).
7. Zhang, Ch. (2002). A 2D hypersingular time-domain traction BEM for transient elastodynamic crack analysis. *Wave Motion*, vol. 35, no. 1, pp. 17–40. https://doi.org/10.1016/S0165-2125(01)00081-6
8. Poruchikov, V. B. (1986). *Metody dinamicheskoy teorii uprugosti* [Methods of the dynamic theory of elasticity]. Moscow: Nauka, 328 p. (in Russian).
9. Popov, V. G. (1993). *Sravneniye poley peremeshcheniy i napryazheniy pri difraktsii uprugikh voln sdviga na razlichnykh defektakh: treshchina i tonkoye zhestkoye vklyucheniye* [Comparison of displacement fields and

stresses in diffraction of elastic shear waves at various defects: crack and thin rigid inclusion]. *Dinamicheskiye sistemy – Dynamical Systems*, iss. 12, pp. 35–41 (in Russian).
10. Vekua, I. N. (1948). *Novyye metody resheniya ellipticheskikh uravneniy* [New methods for solving elliptic equations]. Moscow: OGIZ, 296 p. (in Russian).
11. Belotserkovskiy, S. M. & Lifanov, I. K. (1985). *Chislennyye metody v singulyarnykh integralnykh uravneniyakh* [Numerical methods in singular integral equations]. Moscow: Nauka, 253 p. (in Russian).
12. Kyrylova, O. I. & Mykhaskiv, V. V. (2015). *Ploska dynamichna zadacha dlia tsylindrychnoho tila dovilnoho pererizu z tonkym zhorstkym vkliuchenniam* [A plane dynamic problem for a cylindrical body of arbitrary section with a thin hard inclusion]. *Visnyk Kyivskoho natsionalnoho universytetu. Seriia: fizyko-matematychni nauky –Bulletin of Kyiv National University. Series: physical and mathematical sciences*, no. 5, pp. 167–173 (in Ukrainian).
13. Kyrylova, O. I. & Popov, V. H. (2017). *Napruzhenyi stan u neskinchennomu tsylindri dovilnoho pererizu z tunelnoiu trishchynoiu pry kolyvanniakh v umovakh ploskoi deformatsii* [Stressed state in an infinite cylinder of arbitrary cross section with a tunnel fracture under oscillations under conditions of flat deformation]. *Visnyk Kyivskoho natsionalnoho universytetu. Seriia: fizyko-matematychni nauky –Bulletin of Kyiv National University. Series: physical and mathematical sciences*, no. 3, pp. 71–74 (in Ukrainian).

*Received 11 September 2018*

## Напружений стан порожнинного циліндра з системою тріщин за гармонічних коливань повздовжнього зсуву

**Кирилова О. І., Попов В. Г.**

Національний університет «Одеська морська академія», 65029, Україна, м. Одеса, вул. Дідріхсона, 8

*В роботі розв'язана задача з визначення напруженого стану поблизу тріщин в нескінченному порожнинному циліндрі довільного перерізу під час коливань повздовжнього зсуву. Запропоновано підхід, що дозволяє окремо задовольнити умови на тріщинах та на границях циліндра. Задача зводиться до рівнянь руху в плоскій області з дефектами, обмеженими довільними гладкими замкненими кривими, в умовах антиплоскої деформації. Схема розв'язання базується на використанні розривних розв'язків рівнянь руху пружного середовища зі стрибками переміщень на поверхнях дефектів. Переміщення в циліндрі з дефектами подаються сумою розривних розв'язків, побудованих для кожного дефекту, і невідомої характерної функції, що забезпечує виконання умов гармонічного навантаження на межах тіла. Ця функція розшукується у вигляді комбінації лінійно незалежних розв'язків рівнянь теорії пружності у частотній області з невідомими коефіцієнтами. Сконструйоване подання дає змогу окремо задовольнити крайові умови на поверхні дефектів з отриманням сукупності систем інтегральних рівнянь, що відрізняються тільки правими частинами і не залежать від форми межі тіла. Отримані системи інтегральних рівнянь розв'язуються методом механічних квадратур. Далі задовольняються умови на границях циліндричного тіла, з яких методом колокацій визначаються невідомі коефіцієнти введеної характерної функції. Застосовуючи запропонований підхід, проведено розрахунки коефіцієнтів інтенсивності напружень в околі дефектів, за допомогою яких досліджено вплив на їхні значення частоти та розташування дефектів.*

***Ключові слова**: порожнинний циліндр, гармонічні коливання, коефіцієнти інтенсивності напружень, система тріщин.*

## Література

1. Попов В. Г. Сравнительный анализ дифракционных полей при прохождении упругих волн через дефекты различной природы. *Изв. РАН. Механика твердого тела*. 1995. № 4. С. 99–109.
2. Ang D. D., Knopoff L. Diffraction of scalar elastic waves by a finite strip. *Proc. Math. Sci. USA*. 1964. Vol. 51. No. 4. P. 593–598. https://doi.org/10.1073/pnas.51.4.593
3. Mykhas'kiv V., Zhbadynskyi I., Zhang Ch. Elastodynamic analysis of multiple crack problem in 3-D bi-materials by a BEM. *Int. J. Num. Meth. Biomed. Eng*. 2010. Vol. 26. No. 12. P. 1934–1946. https://doi.org/10.1002/cnm.1285
4. Попов В. Г. Взаимодействие плоских упругих волн с системами радиальных дефектов. *Изв. РАН. Механика твердого тела*. 1999. № 4. С. 118–129.
5. Chirino F., Domingues J. Dynamic analysis of cracks using boundary element method. *Eng. Fracture Mech.* 1989. Vol. 34. No. 5–6. P. 1051–1061. https://doi.org/10.1016/0013-7944(89)90266-X
6. Бобылев А. А., Доброва Ю. А. Применение метода граничных элементов к расчету вынужденных колебаний упругих тел конечных размеров с трещинами. *Вестн. Харьк. нац. ун-та*. 2003. № 590. Вып. 1. С. 49–54.

7. Zhang Ch. A 2D hypersingular time-domain traction BEM for transient elastodynamic crack analysis. *Wave Motion*. 2002. Vol. 35. No. 1. P. 17–40. https://doi.org/10.1016/S0165-2125(01)00081-6
8. Поручиков В. Б. Методы динамической теории упругости. М.: Наука, 1986. 328 с.
9. Попов В. Г. Сравнение полей перемещений и напряжений при дифракции упругих волн сдвига на различных дефектах: трещина и тонкое жесткое включение. *Динам. системы*. 1993. Вып.12. С. 35–41.
10. Векуа И. Н. Новые методы решения эллиптических уравнений. М.: ОГИЗ, 1948. 296 с.
11. Белоцерковский С. М, Лифанов И. К. Численные методы в сингулярных интегральных уравнениях. М.: Наука, 1985. 253 с.
12. Кирилова О. І., Михаськів В. В. Плоска динамічна задача для циліндричного тіла довільного перерізу з тонким жорстким включенням. *Вісн. Київ. нац. ун-ту. Сер. Фіз.-мат. науки*. 2015. № 5. С. 167–173.
13. Кирилова О. І., Попов В. Г. Напружений стан у нескінченному циліндрі довільного перерізу з тунельною тріщиною при коливаннях в умовах плоскої деформації. *Вісн. Київ. нац. ун-ту. Сер. Фіз-мат. науки*. 2017. № 3. С. 71–74.


**DOI: https://doi.org/10.15407/pmach2019.01.024**

UDC 539.3

# MAJOR STRESS-STRAIN STATE OF DOUBLE SUPPORT MULTILAYER BEAMS UNDER CONCENTRATED LOAD
## Part 2. Model Implementation And Calculation Results

**Stanislav B. Kovalchuk**
stanislav.kovalchuk@pdaa.edu.ua
ORCID: 0000-0003-4550-431X

**Oleksii V. Goryk**
ORCID: 0000-0002-2804-5580

Poltava State Agrarian Academy
1/3, Skovorody St., Poltava, 36003, Ukraine

*The development of composite technologies contributes to their wide introduction into the practice of designing modern different-purpose structures. Reliable prediction of the stress-strain state of composite elements is one of the conditions for creating reliable structures with optimal parameters. Analytical theories for determining the stress-strain state of multilayer rods (bars, beams) are significantly inferior in development to those for composite plates and shells, although their core structural elements are most common. The purpose of this paper is to design an analytical model for bending double support multilayer beams under a concentrated load, with the model based on the previously obtained elasticity theory solution for a multi-layer cantilever. The second part of the article contains examples of the implementation of the model for bending double-support multi-layer beams under a concentrated load, with the model constructed in the first part of the article. Using this model, solutions to the problems of bending multilayer beams with different types of fixation of their extreme cross-sections were obtained. The resultant relations were approbated using test problems for determining the deflections of homogeneous composite double-support beams with different combinations of fixation, as well as in determining the stresses and displacements of a four-layer beam with a combination of a rigid and hinged fixation at its ends. The results obtained have a slight discrepancy with the simulation results by the finite element method (FEM) and the calculation by the iterative model for bending composite bars, even for relatively short beams. In addition, it is shown that the neglect of the shear amenability of layer materials results in large errors in determining the deflections, and in the case of statically indefinable beams, reactive forces and stresses. The approach used in the construction of the model can be extended to the case of beams with arbitrary numbers of concentrated forces and intermediate supports, and to calculate multilayer beams with different rigidity of their design sections.*

***Keywords***: *multilayer beam, orthotropic layer, concentrated load, deflection, stresses, displacements.*

### Introduction

The mechanics of deformation of composite multilayer plates and shells is the subject of a large number of fundamental scientific works [1–8]. The deformation of composite rods (bars, beams) is less studied, although such structural elements are most common.

When a problem of bending composite beams is solved, there is a wide spread use of refined models, in particular, constructed by an iterative method [9–11]. Such models are quite universal, however, they are very cumbersome and difficult for practical use at high refinement steps. At the same time, exact solutions for